a

Gene	Chr	Position	Variant type	Reference	Variant	dbSNP v135	Coding change	Prediction	Segregaion analysis
TTN	2	179 410777	Missense	G	T	Not present	W30088L	Probably damaging	Segregating
IKBKB	8	42 188 457	Missense	C	T	rs138183879	T742M	Benign	Non-segregating

b

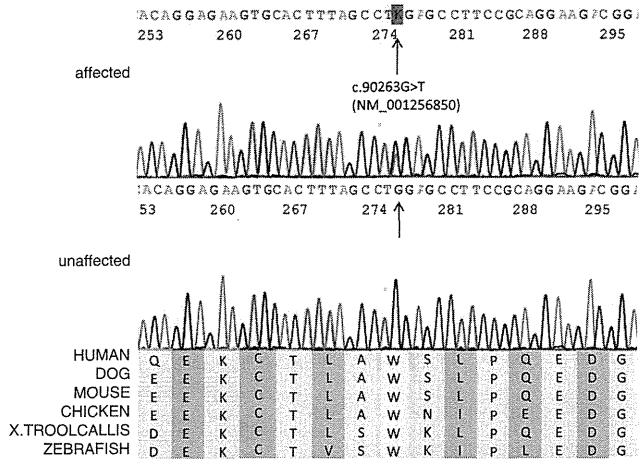

Figure 4 Identified mutations by exome sequencing. (**a**) We performed segregation analysis of two candidates. (**b**) The identified *TTN* mutation and its conservation among species. Sanger sequencing confirmed the heterozygous G to T substitution (indicated by the arrow) at the position chr2;179 410 777, which corresponds to c.90263G>T in exon 293 (NM_001256850.1). The substitution leads to p.W30088L (NP_001243779.1), and this amino acid is conserved among species.

These values were not compatible with the assumption that MFM was a rare disease and showed complete penetrance in this family. The allele frequency of rs138183879 was not available in dbSNP135, and this SNV was in the candidate region on chromosome 8 based on linkage analysis.

We then performed a segregation analysis on the two candidates, the novel mutation c.90263G>T in *TTN* and rs138183879 in *IKBKB*, through Sanger sequencing in 10 family members (A–J in Figure 1; Figure 4a). The rs138183879 SNP was not found in individual J, that is, it was not segregated with the disease in this family. In contrast, the novel mutation c.90263G>T in *TTN* was detected in all patients ($n=5$) and not detected in any of the unaffected family members ($n=5$) or 191 ethnically matched control subjects (382 chromosomes). These results suggested that this rare mutation in *TTN* segregated with the disease in this family.

DISCUSSION

In this study, we found that a novel missense mutation in *TTN* segregated with MFM in a large Japanese family. The identified c.90263G>T mutation in *TTN* (NM_001256850) was considered to be the genetic cause of MFM in our family, because (1) exome sequencing revealed that this was the best candidate mutation after filtering SNPs and indels, (2) this mutation is located in a region on chromosome 2 shared by affected family members, (3) the segregation with MFM was confirmed by Sanger sequencing, (4) this mutation was not detected in 191 control individuals, (5) this mutation was predicted to alter highly conserved amino acids (Figure 4b) and (6) *TTN* encodes a Z-disc-binding molecule called titin, which is similar to all of the previously identified causative genes for MFMs, which also encode Z-disc-associated molecules.

Recently, three mutations in *TTN* have been reported as the causes of hereditary myopathy with early respiratory failure (HMERF, MIM #603689),[11–16] which has similar muscle pathology to MFMs. The identified novel missense mutation c.90263G>T in our study was located on the same exon as recently reported HMERF mutations: c.90272C>T in a Portuguese family[16] and c.90315T>C in Swedish and English families[14,15] (Table 2). This finding suggests the possibility that our family can be recognized as having HMERF from a clinical aspect.

Compared with symptoms described in the past three reports on HMERF (also see Table 2), our patients have common features, such as autosomal dominant inheritance, early respiratory failure, the absence of clinically apparent cardiomyopathy, normal to mild elevation of serum CK and histological findings compatible with MFM. Early involvement of the tibialis anterior is also common, except for the Portuguese family, who reported isolated respiratory insufficiency and a milder presentation of HMERF. Thus, our family shares major clinical manifestations with patients with HMERF, suggesting that the identified mutation is novel for MFM and HMERF.

To date, mutations in *TTN* have been identified in skeletal myopathy and cardiomyopathy.[17,18] The relationship between the variant positions on *TTN* and phenotypes accompanied by skeletal or respiratory muscle involvement is summarized in Table 2. Titin is a large protein (4.20 MDa) that extends from the Z-disk to the M-line within the sarcomere, and it is composed of four major domains: Z-disc, I-band, A-band and M-line (Figure 5). All four HMERF mutations detected by other groups and our study were consistently located in the A-band domain, while mutations in tibial muscular dystrophy (TMD) (MIM #600334),[19–24] limb-girdle muscular dystrophy type 2J (LGMD2J) (#608807)[19,25] and early-onset myopathy with fatal cardiomyopathy (#611705)[26] were located in the M-line domain. HMERF and TMD have some common clinical characteristics, such as autosomal dominant inheritance with onset in adulthood and strong involvement of the tibialis anterior muscle.

Table 2 Previously reported TTN mutations with skeletal and/or respiratory muscle involvement

Phenotype	*LGMD*	*HMERF*	*Our family*	*HMERF*	*HMERF*	*TMD*	*TMD*	*LGMD2J*	*TMD*	*TMD*	*TMD*	*TMD*	*TMD*	*Early-onset myopathy with fatal cardiomyopathy*	*Early-onset myopathy with fatal cardiomyopathy*
Reported by	Vasli *et al.*[16]	Ohlsson *et al.*,[14] Pfeffer *et al.*[15]	Abe *et al.*[5]	Vasli *et al.*[16]	Edstrom *et al.*,[12] Nicolao, *et al.*[11] Lang e *et al.*[13]	Hackman *et al.*[23]	Udd *et al.*,[20] Hackman *et al.*[19]	Udd *et al.*,[25] Hackman *et al.*[19]	Pollazzon *et al.*[24]	Van den Bergh *et al.*[22]	Seze *et al.*,[21] Hackman *et al.*[19]	Hackman *et al.*[23]	Hackman *et al.*[23]	Carmignac *et al.*[26]	Carmignac *et al.*[26]
Mutation identified in Nucleotide (NM_001256850.1)	2012 c.3100G>A, c.52024G>A	2012 c.90315T>C	2012 c.90263G>T	2012 c.90272C>T	2005 c.97348C>T	2008 c.102724delT	2002 102857_102867 del11ins11	2002 102857_102867 del11ins11	2010 c.102914A>C	2003 c.102917T>A	2002 c.102944T>C	2008 c.102966delA	2008 c.102967C>T	2007 g.289385del ACCAAGTG	2007 g.291297delA
Protein (NP_001243779.1)	p.V1034M, p.A17342T	p.C30071R	p.W30088L	p.P30091L	p.R32450W				p.H34305P	p.I34306N	p.L34315P		p.Q34323X		
Domain	I-band, A-band	A-band (Fn3)	A-band (Fn3)	A-band (Fn3)	A-band (kinase)	M-line	M-line	M-line	M-line	M-line	M-line	M-line	M-line	M-line	M-line
Population	French	Swedish English	Japanese	Portuguese	Swedish	French	Finnish	Finnish	Italian	Belgian	French	Spanish	French	Sudanese	Moroccan
Inheritance	AR	AD	AD	AD	AD	AD	AD	AR	AD	AD	AD	AD	AD	Consanguineous siblings	Consanguineous siblings
Onset	35	33–71	27–45	46	20–50s	20–30s	35–55	20–30s	50–60s	47	45	40–50s	30s	Neonatal	Infant-early childhood
Skeletal muscles															
Major	Proximal UL and LL	TA, PL, EDL, ST	TA, ST	No	TA, neck flexor, proximals	TA, GA,HAM, pelvic	TA	All proximals	TA	TA	TA	TA	TA, HAM, pelvic	General muscle weakness and hypotonia	Psoas, TA, GA, peroneus
Minor		Neck flexor	Cervical, shoulder girdles, intercostals, proximal limb			QF				EDL, peroneal, TP	GA, femoral, scapular	HAM, GA	GA, distal UL		QF, proximal UL, neck, facial, trunk flexor
Spared			Facial			Proximal UL	Facial, UL, proximals	Facial		UL, proximal LL	Facial	UL	Proximal UL, QF		
Cardiac muscles	ND	No	No	ND	ND	ND	No	No	ND	ND	ND	ND	ND	DCM, onset; in the first decade	DCM, onset; 5–12 years old
Respiratory failure	ND	Yes, within 5–8 years	Yes, within 7 years	Isolated respiratory failure	Yes, as first presentation	ND	ND	ND	ND	ND	ND	ND	ND	ND	ND
Muscle pathologic features	ND	Inclusion bodies (major) and RVs (minor)	Cytoplasmic bodies (major) and RVs (minor)	Cytoplasmic bodies	Cytoplasmic bodies, positive for rhodamine-conjugated phalloidin	Dystrophic pattern without vacuoles	Nonspecific dystrophic change	Nonspecific dystrophic change, loss of calpain-3	Dystrophic pattern with RVs	Nonspecific, RV	Nonspecific	Dystrophic pattern with RVs	Nonspecific	Minicore-like lesions and abundant central nuclei	Minicore-like lesions and abundant central nuclei

Abbreviations: AD, autosomal dominant; AR, autosomal recessive; DCM, dilated cardiomyopathy; EDL, extensor digitorum longus; GA, gastrocnemius; HAM, hamstrings; LL, lower limb; ND, not described; no, no involvement; PL, peroneus longus; QF, quadriceps femoris; RV, rimmed vacuole;
ST, semitendinosus; TA, tibialis anterior; TMD, tibial muscular dystrophy; TP, tibialis posterior; UL, upper limb.

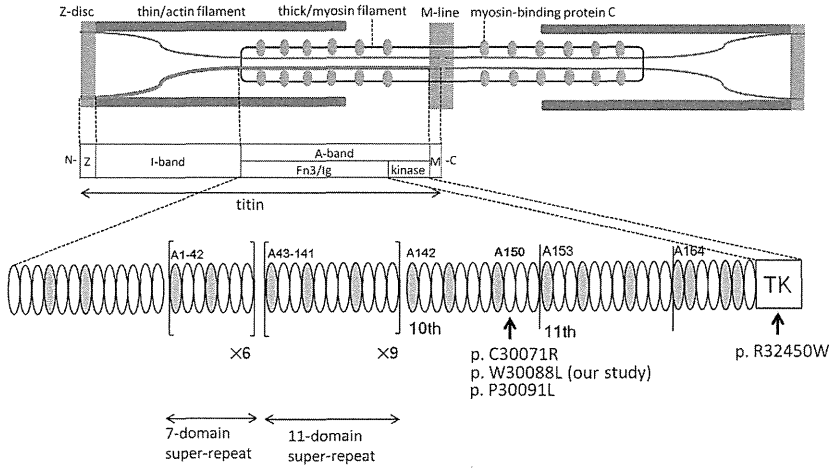

Figure 5 Structure of titin and mutation distribution in the A-band domain. Human *TTN* was mapped to 2q31.2. *TTN* is 294 kb and is composed of 363 exons that code for a maximum of 38 138 amino-acid residues and a 4.20-MDa protein[32] called titin. Titin is expressed in the cardiac and skeletal muscles and spans half the sarcomere, with its N-terminal at the Z-disc and the C-terminal at the M-line.[33] Titin is composed of four major domains: Z-disc, I-band, A-band and M-line. I-band regions of titin are thought to make elastic connections between the thick filament (that is, myosin filament) and the Z-disc within the sarcomere, whereas the A-band domain of titin seems to be bound to the thick filament, where it may regulate filament length and assembly.[34] The gray and white ellipses indicate an Ig-like domain and fibronectin type 3 domain, respectively. Our mutation (p.W30088L) and the neighboring two mutations (that is, p.C30071R and p.P30091L) were all located in the 6th Fn3 domain in the 10th domain of large super-repeats. A full color version of this figure is available at the *Journal of Human Genetics* journal online.

In contrast, one of the distinctive features of TMD is that early respiratory failure has not been observed in patients with TMD. Histological findings of TMD usually do not include CBs but show nonspecific dystrophic change. The underlying pathogenic processes explaining why mutations on these neighboring domains share some similarities but also some differences are unknown.

Three of four HMERF mutations in the A-band domain are located in the fibronectin type 3 and Ig-like (Fn3/Ig) domain, and one of four HMERF mutations is located in the kinase domain (Table 2, also see Figure 5). The missense mutation c.97348C>T in the kinase domain was the first reported HMERF mutation. It has been shown that the kinase domain has an important role in controlling muscle gene expression and protein turnover via the neighbor of BRCA1 gene-1-muscle-specific RING finger protein-serum response transcription factor pathway.[13] Moreover, the Fn3/Ig domain is composed of two types of super-repeats: six consecutive copies of 7-domain super-repeat at the N-terminus and 11 consecutive copies of 11-domain super-repeat at the C-terminus.[27–29] These super-repeats are highly conserved among species and muscles. Our identified mutation (c.90263G>T) and the neighboring two mutations (that is, c.90272C>T and c.90315T>C shown in Table 2) were all located on the 6th Fn3 domain in the 10th copy of 11-domain super-repeat (that is, A150 domain[30]) (Figure 5). Although some Fn3 domains are proposed to be the putative binding site for myosin,[31] the role with the majority of Fn3 domains, how it supports the structure of each repeat architecture, and the identity of its binding partner have not been fully elucidated. Our findings suggested that the Fn3 domain, in which mutations clustered, has critical roles in the pathogenesis of HMERF, although detailed mechanisms of pathogenesis remain unknown.

In conclusion, we have identified a novel disease-causing mutation in *TTN* in a family with MFM that was clinically compatible with HMERF. Because of its large size, global mutation screening of *TTN* has been difficult. Mutations in *TTN* may be detected by massively parallel sequencing in more patients with MFMs, especially in patients with early respiratory failure. Further studies are needed to understand the genotype–phenotype correlations in patients with mutations in *TTN* and the molecular function of titin.

ACKNOWLEDGEMENTS

We thank the patients and their family. We are grateful to Yoko Tateda, Kumi Kato, Naoko Shimakura, Risa Ando, Riyo Takahashi, Miyuki Tsuda, Nozomi Koshita, Mami Kikuchi and Kiyotaka Kuroda for their technical assistance. We also acknowledge the support of the Biomedical Research Core of Tohoku University Graduate School of Medicine. This work was supported by a grant of Research on Applying Health Technology provided by the Ministry of Health, Labor and Welfare to YM, an Intramural Research Grant (23-5) for Neurological and Psychiatric Disorders of NCNP and JSPS KAKENHI Grant number 24659421.

1 Nakano, S., Engel, A. G., Waclawik, A. J., Emslie-Smith, A. M. & Busis, N. A. Myofibrillar myopathy with abnormal foci of desmin positivity. I. Light and electron microscopy analysis of 10 cases. *J. Neuropathol. Exp. Neurol.* **55,** 549–562 (1996).
2 Olive, M., Odgerel, Z., Martinez, A., Poza, J. J., Bragado, F. G., Zabalza, R. J. *et al.* Clinical and myopathological evaluation of early- and late-onset subtypes of myofibrillar myopathy. *Neuromuscul. Disord.* **21,** 533–542 (2011).
3 Olive, M., Goldfarb, L. G., Shatunov, A., Fischer, D. & Ferrer, I. Myotilinopathy: refining the clinical and myopathological phenotype. *Brain* **128,** 2315–2326 (2005).
4 Selcen, D. & Engel, A. G. Myofibrillar myopathy caused by novel dominant negative alpha B-crystallin mutations. *Ann. Neurol.* **54,** 804–810 (2003).
5 Abe, K., Kobayashi, K., Chida, K., Kimura, N. & Kogure, K. Dominantly inherited cytoplasmic body myopathy in a Japanese kindred. *Tohoku. J. Exp. Med.* **170,** 261–272 (1993).
6 Abecasis, G. R., Cherny, S. S., Cookson, W. O. & Cardon, L. R. Merlin–rapid analysis of dense genetic maps using sparse gene flow trees. *Nat. Genet.* **30,** 97–101 (2002).
7 Li, H. & Durbin, R. Fast and accurate short read alignment with Burrows-Wheeler transform. *Bioinformatics* **25,** 1754–1760 (2009).
8 McKenna, A., Hanna, M., Banks, E., Sivachenko, A., Cibulskis, K., Kernytsky, A. *et al.* The Genome Analysis Toolkit: a MapReduce framework for analyzing next-generation DNA sequencing data. *Genome. Res.* **20,** 1297–1303 (2010).
9 Wang, K., Li, M. & Hakonarson, H. ANNOVAR: functional annotation of genetic variants from high-throughput sequencing data.. *Nucleic Acids Res.* **38,** e164 (2010).
10 Adzhubei, I. A., Schmidt, S., Peshkin, L., Ramensky, V. E., Gerasimova, A., Bork, P. *et al.* A method and server for predicting damaging missense mutations. *Nat. Methods* **7,** 248–249 (2010).
11 Nicolao, P., Xiang, F., Gunnarsson, L. G., Giometto, B., Edstrom, L., Anvret, M. *et al.* Autosomal dominant myopathy with proximal weakness and early respiratory muscle involvement maps to chromosome 2q. *Am. J. Hum. Genet.* **64,** 788–792 (1999).

12 Edstrom, L., Thornell, L. E., Albo, J., Landin, S. & Samuelsson, M. Myopathy with respiratory failure and typical myofibrillar lesions. *J. Neurol. Sci.* **96,** 211–228 (1990).
13 Lange, S., Xiang, F., Yakovenko, A., Vihola, A., Hackman, P., Rostkova, E. *et al.* The kinase domain of titin controls muscle gene expression and protein turnover. *Science* **308,** 1599–1603 (2005).
14 Ohlsson, M., Hedberg, C., Bradvik, B., Lindberg, C., Tajsharghi, H., Danielsson, O. *et al.* Hereditary myopathy with early respiratory failure associated with a mutation in A-band titin. *Brain* **135,** 1682–1694 (2012).
15 Pfeffer, G., Elliott, H. R., Griffin, H., Barresi, R., Miller, J., Marsh, J. *et al.* Titin mutation segregates with hereditary myopathy with early respiratory failure. *Brain* **135,** 1695–1713 (2012).
16 Vasli, N., Bohm, J., Le Gras, S., Muller, J., Pizot, C., Jost, B. *et al.* Next generation sequencing for molecular diagnosis of neuromuscular diseases. *Acta. Neuropathol.* **124,** 273–283 (2012).
17 Kontrogianni-Konstantopoulos, A., Ackermann, M. A., Bowman, A. L., Yap, S. V. & Bloch, R. J. Muscle giants: molecular scaffolds in sarcomerogenesis. *Physiol. Rev.* **89,** 1217–1267 (2009).
18 Ottenheijm, C. A. & Granzier, H. Role of titin in skeletal muscle function and disease. *Adv. Exp. Med. Biol.* **682,** 105–122 (2010).
19 Hackman, P., Vihola, A., Haravuori, H., Marchand, S., Sarparanta, J., De Seze, J. *et al.* Tibial muscular dystrophy is a titinopathy caused by mutations in TTN, the gene encoding the giant skeletal-muscle protein titin. *Am. J. Hum. Genet.* **71,** 492–500 (2002).
20 Udd, B., Partanen, J., Halonen, P., Falck, B., Hakamies, L., Heikkila, H. *et al.* Tibial muscular dystrophy. Late adult-onset distal myopathy in 66 Finnish patients. *Arch. Neurol.* **50,** 604–608 (1993).
21 de Seze, J., Udd, B., Haravuori, H., Sablonniere, B., Maurage, C. A., Hurtevent, J. F. *et al.* The first European family with tibial muscular dystrophy outside the Finnish population. *Neurology* **51,** 1746–1748 (1998).
22 Van den Bergh, P. Y., Bouquiaux, O., Verellen, C., Marchand, S., Richard, I., Hackman, P. *et al.* Tibial muscular dystrophy in a Belgian family. *Ann. Neurol.* **54,** 248–251 (2003).
23 Hackman, P., Marchand, S., Sarparanta, J., Vihola, A., Penisson-Besnier, I., Eymard, B. *et al.* Truncating mutations in C-terminal titin may cause more severe tibial muscular dystrophy (TMD). *Neuromuscul. Disord.* **18,** 922–928 (2008).
24 Pollazzon, M., Suominen, T., Penttila, S., Malandrini, A., Carluccio, M. A., Mondelli, M. *et al.* The first Italian family with tibial muscular dystrophy caused by a novel titin mutation. *J. Neurol.* **257,** 575–579 (2010).
25 Udd, B., Rapola, J., Nokelainen, P., Arikawa, E. & Somer, H. Nonvacuolar myopathy in a large family with both late adult onset distal myopathy and severe proximal muscular dystrophy. *J. Neurol. Sci.* **113,** 214–221 (1992).
26 Carmignac, V., Salih, M. A., Quijano-Roy, S., Marchand, S., Al Rayess, M. M., Mukhtar, M. M. *et al.* C-terminal titin deletions cause a novel early-onset myopathy with fatal cardiomyopathy. *Ann. Neurol.* **61,** 340–351 (2007).
27 Labeit, S., Barlow, D. P., Gautel, M., Gibson, T., Holt, J., Hsieh, C. L. *et al.* A regular pattern of two types of 100-residue motif in the sequence of titin. *Nature* **345,** 273–276 (1990).
28 Labeit, S. & Kolmerer, B. Titins: giant proteins in charge of muscle ultrastructure and elasticity. *Science* **270,** 293–296 (1995).
29 Tskhovrebova, L., Walker, M. L., Grossmann, J. G., Khan, G. N., Baron, A. & Trinick, J. Shape and flexibility in the titin 11-domain super-repeat. *J. Mol. Biol.* **397,** 1092–1105 (2010).
30 Bucher, R. M., Svergun, D. I., Muhle-Goll, C. & Mayans, O. The structure of the FnIII Tandem A77-A78 points to a periodically conserved architecture in the myosin-binding region of titin. *J. Mol. Biol.* **401,** 843–853 (2010).
31 Muhle-Goll, C., Habeck, M., Cazorla, O., Nilges, M., Labeit, S. & Granzier, H. Structural and functional studies of titin's fn3 modules reveal conserved surface patterns and binding to myosin S1–a possible role in the Frank-Starling mechanism of the heart. *J. Mol. Biol.* **313,** 431–447 (2001).
32 Bang, M. L., Centner, T., Fornoff, F., Geach, A. J., Gotthardt, M., McNabb, M. *et al.* The complete gene sequence of titin, expression of an unusual approximately 700-kDa titin isoform, and its interaction with obscurin identify a novel Z-line to I-band linking system. *Circ. Res.* **89,** 1065–1072 (2001).
33 Maruyama, K., Yoshioka, T., Higuchi, H., Ohashi, K., Kimura, S. & Natori, R. Connectin filaments link thick filaments and Z lines in frog skeletal muscle as revealed by immunoelectron microscopy. *J. Cell. Biol.* **101,** 2167–2172 (1985).
34 Guo, W., Bharmal, S. J., Esbona, K. & Greaser, M. L. Titin diversity–alternative splicing gone wild. *J. Biomed. Biotechnol.* **2010,** 753675 (2010).

Supplementary Information accompanies the paper on Journal of Human Genetics website (http://www.nature.com/jhg)

Molecular Genetics and Metabolism xxx (2012) xxx–xxx

Contents lists available at SciVerse ScienceDirect

Molecular Genetics and Metabolism

journal homepage: www.elsevier.com/locate/ymgme

Simple and rapid genetic testing for citrin deficiency by screening 11 prevalent mutations in *SLC25A13*

Atsuo Kikuchi [a,*], Natsuko Arai-Ichinoi [a], Osamu Sakamoto [a], Yoichi Matsubara [b], Takeyori Saheki [c,1], Keiko Kobayashi [d], Toshihro Ohura [e], Shigeo Kure [a]

[a] Department of Pediatrics, Tohoku University Graduate School of Medicine, 1-1 Seiryo-machi, Aoba-ku, Sendai, Miyagi 980-8574, Japan
[b] Department of Medical Genetics, Tohoku University School of Medicine, 1-1 Seiryo-machi, Aoba-ku, Sendai, Miyagi 980-8574, Japan
[c] Institute for Health Sciences, Tokushima Bunri University, 180 Yamashiro-cho, Tokushima 770-8514, Japan
[d] Department of Molecular Metabolism and Biochemical Genetics, Kagoshima University, Kagoshima 890-8544, Japan
[e] Division of Pediatrics, Sendai City Hospital, 3-1 Shimizukoji, Wakabayashi-ku, Sendai, Miyagi 984-8501, Japan

ARTICLE INFO

Article history:
Received 13 November 2011
Received in revised form 29 December 2011
Accepted 30 December 2011
Available online xxxx

Keywords:
Citrin deficiency
Genetic diagnosis
Rapid diagnosis
Expanded newborn screening
SLC25A13

ABSTRACT

Citrin deficiency is an autosomal recessive disorder caused by mutations in the *SLC25A13* gene and has two disease outcomes: adult-onset type II citrullinemia and neonatal intrahepatic cholestasis caused by citrin deficiency. The clinical appearance of these diseases is variable, ranging from almost no symptoms to coma, brain edema, and severe liver failure. Genetic testing for *SLC25A13* mutations is essential for the diagnosis of citrin deficiency because chemical diagnoses are prohibitively difficult. Eleven *SLC25A13* mutations account for 95% of the mutant alleles in Japanese patients with citrin deficiency. Therefore, a simple test for these mutations is desirable. We established a 1-hour, closed-tube assay for the 11 *SLC25A13* mutations using real-time PCR. Each mutation site was amplified by PCR followed by a melting-curve analysis with adjacent hybridization probes (HybProbe, Roche). The 11 prevalent mutations were detected in seven PCR reactions. Six reactions were used to detect a single mutation each, and one reaction was used to detect five mutations that are clustered in a 21-bp region in exon 17. To test the reliability, we used this method to genotype blind DNA samples from 50 patients with citrin deficiency. Our results were in complete agreement those obtained using previously established methods. Furthermore, the mutations could be detected without difficulty using dried blood samples collected on filter paper. Therefore, this assay could be used for newborn screening and for facilitating the genetic diagnosis of citrin deficiency, especially in East Asian populations.

© 2012 Elsevier Inc. All rights reserved.

1. Introduction

Citrin deficiency is an autosomal recessive disorder that results from mutations in the *SLC25A13* gene [1] and causes two diseases: adult-onset type II citrullinemia (CTLN2; OMIM #603471) and neonatal intrahepatic cholestasis caused by citrin deficiency (NICCD; OMIM#605814) [1–4]. The clinical appearance of these diseases is variable and ranges from almost no symptoms to coma, brain edema, and severe liver failure requiring transplantation [5–8]. In a study of patients with NICCD, only 40% of individuals were identified by newborn screenings to have abnormalities, such as hypergalactosemia, hypermethioninemia, and hyperphenylalaninemia [9]. Other patients were referred to hospitals with suspected neonatal hepatitis or biliary atresia, due to jaundice or discolored stool [9]. Hypercitrullinemia was not observed in all patients [9]. Mutation analysis of *SLC25A13* is indispensable because of the difficulties associated with the chemical diagnosis of citrin deficiency. The *SLC25A13* mutation spectrum in citrin deficiency is heterogeneous, and more than 31 mutations of *SLC25A13* have been identified to date [1,10–18]. However, there are several predominant mutations in patients from East Asia. As shown in Table 1, 6 prevalent mutations account for 91% of the mutant alleles in the Japanese population [12,19]. Five additional mutations also occur within a 21-bp cluster in exon 17 (Table 1 and Fig. 1D). The six prevalent mutations, together with the five mutations in exon 17, account for 95% of the mutant alleles in Japan [12,19].

Several different methods, such as direct sequencing, PCR restriction fragment length polymorphism (PCR-RFLP), and denaturing high performance liquid chromatography (DHPLC), are currently used for the detection of mutations in *SLC25A13* [1,10–14,19]. However, these methods are too complex for clinical use. Direct sequencing is a standard but cumbersome method. The PCR-RFLP method is

Abbreviations: CTLN2, adult-onset type II citrullinemia; FRET, fluorescence resonance energy transfer; HRM, high resolution melting; NICCD, neonatal intrahepatic cholestasis caused by citrin deficiency; Tm, melting temperature.

* Corresponding author. Fax: +81 22 717 7290.
E-mail address: akikuchi-thk@umin.ac.jp (A. Kikuchi).
[1] Present address: Institute of Resource Development and Analysis, Kumamoto University, Kumamoto 860-0811, Japan.

1096-7192/$ – see front matter © 2012 Elsevier Inc. All rights reserved.
doi:10.1016/j.ymgme.2011.12.024

Please cite this article as: A. Kikuchi, et al., Simple and rapid genetic testing for citrin deficiency by screening 11 prevalent mutations in *SLC25A13*, Mol. Genet. Metab. (2012), doi:10.1016/j.ymgme.2011.12.024

ARTICLE IN PRESS

Table 1
Seven primer/probe sets and 11 targeted mutations of *SLC25A13*.

Primer/probe set	Mutation		Location	Nucleotide change	Effects of mutations	Allele frequency*[19]	References
A	Mutation [I]	:851del4	exon 9	c.851_854delGTAT	p.R284fs(286X)	33.2%	[1]
B	Mutation [II]	:g.IVS11+1G>A	intron 11	c.1019_1177del	p.340_392del	37.6%	[1]
C	Mutation [III]	:1638ins23	exon 16	c.1638_1660dup	p.A554fs(570X)	3.4%	[1]
D	Mutation [IV]	:S225X	exon 7	c.675C>A	p.S225X	5.3%	[1]
E	Mutation [V]	:g.IVS13+1G>A	intron 13	c.1231_1311del	p.411_437del	8.2%	[1]
F	Mutation [XIX]	:IVS16ins3kb	intron 16	c. aberrant RNA	p.A584fs(585X)	4.6%	[19]
G	Mutation [VI]	:1800ins1	exon 17	c.1799_1800insA	p.Y600X	1.3%	[10]
	Mutation [VII]	:R605X	exon 17	c.1813C>T	p.R605X	0.90%	[10]
	Mutation [VIII]	:E601X	exon 17	c.1801G>T	p.E601X	1.2%	[11]
	Mutation [IX]	:E601K	exon 17	c.1801G>A	p.E601K	0.30%	[11]
	Mutation [XXI]	:L598R	exon 17	c.1793T>G	p.L598R	0%	[15]
						Total 95.1%	

* The frequency of each mutant allele among Japanese patients with citrin deficiency.

complicated and can lead to genotyping errors, due to incomplete digestion by the restriction enzymes. DHPLC is time-consuming and requires expensive equipment. Thus, there is a strong need for the development of a simple test for these mutations.

The goal of this study was to establish a rapid and simple test for the detection of the 11 most common *SLC25A13* mutations. We adopted the HybProbe format (Roche) for the detection of the mutations using real-time PCR followed by a melting-curve analysis with adjacent hybridization probes [20,21]. This assay can be completed in less than 1 h and has the advantage of being a closed-tube assay. The fundamental process for detecting point mutations using the HybProbe assay is presented in Fig. 1A. The 11 prevalent mutations contain not only point mutations but also include a 4-bp deletion and insertions of 1-bp, 23-bp and 3-kb genomic fragments (Table 1 and Fig. 1). Careful design of the PCR primers and HybProbes enabled us to test for these various *SLC25A13* mutations.

2. Methods

2.1. Subjects

CTLN2 and NICCD were diagnosed, as previously described [9,10,19,22–24]. Genomic DNA of the patients was obtained from peripheral blood leukocytes using the DNeasy blood kit (Qiagen Inc., Valencia, CA, USA). Genomic DNA was purified from filter paper blood samples using the ReadyAmp Genomic DNA Purification System (Promega, Madison, WI, USA). Mutations in these DNA samples were analyzed at Kagoshima University using a combination of PCR with or without restriction enzyme digestion or by direct sequencing, as previously described [1,10–14,19]. Another set of samples was obtained from 420 healthy volunteers (mainly from Miyagi prefecture in the northeastern region of Japan) at Tohoku University. Genomic DNA from leukocytes was extracted, as described above.

2.2. Detection of seven prevalent mutations in SLC25A13 using the HybProbe assay

HybProbe probes comprise a pair of donor and acceptor oligonucleotide probes designed to hybridize adjacent to their target sites in an amplified DNA fragment [20,21]. The donor probes are labeled at their 3′ end with fluorescein isothiocyanate (FITC), whereas the acceptor probes are labeled at their 5′ end with LC Red640; these acceptor probes are phosphorylated at their 3′ end to prevent extension by the DNA polymerase. When two probes hybridize to the amplicon, the fluorescent dyes are located within 5 bases of each other, which allows fluorescence resonance energy transfer (FRET) between the excited FITC and the LC Red640; this process emits light that can be quantified by real-time PCR. Following PCR amplification, a melting-peak analysis is performed. The melting peak is produced by the reporter probe, which has a lower melting temperature (Tm) than the other probe, called the anchor probe. As the reporter melts from the target, the fluorophores are separated, and the FRET ceases. The Tm of the reporter probe determines the reaction

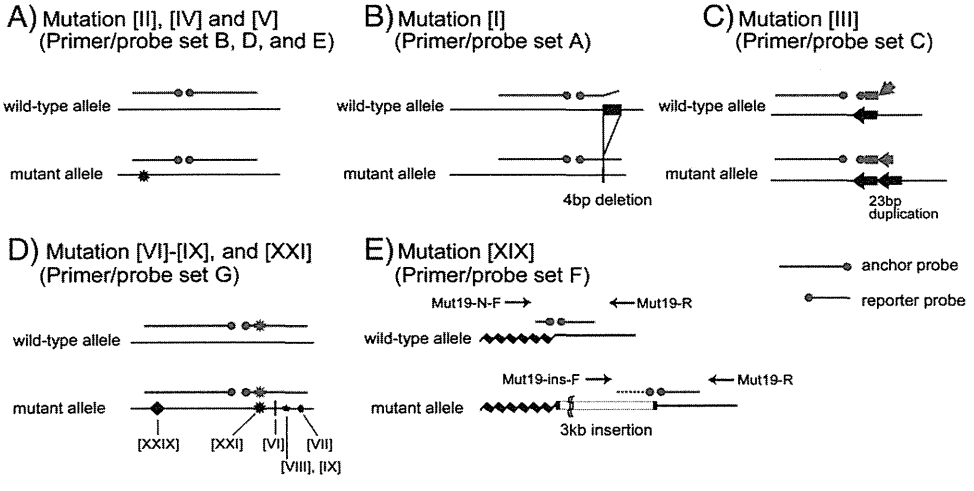

Fig. 1. Principle of *SLC25A13* mutation detection by melting-curve analysis with the HybProbe assay. In primer/probe sets A–E, and G, PCR was performed with a pair of primers, whereas in primer/probe set F, two forward primers and one common reverse primer were used for the amplification of both wild-type and mutant alleles. Note that mutation [XXIX], located on the anchor probe of primer/probe set G, is a non-target mutation.

Please cite this article as: A. Kikuchi, et al., Simple and rapid genetic testing for citrin deficiency by screening 11 prevalent mutations in *SLC25A13*, Mol. Genet. Metab. (2012), doi:10.1016/j.ymgme.2011.12.024

specificity (i.e., binding of the probe to a perfectly matched sequence rather than to regions with sequence mismatches).

Seven primer/probe sets were designed for this study. Fig. 1 shows a schematic diagram of the strategy for mutation detection using these primer/probe sets. Tables 1 and 2 list the primer/probe sets and corresponding sequences and primer concentrations that were used to target the 11 mutations. Primer/probe sets A, B, C, D, E, and F were designed to detect mutations [I], [II], [III], [IV], [V], and [XIX], respectively. Primer/probe set G was designed to detect the five mutations clustered on exon 17: mutations [VI], [VII], [VIII], [IX], and [XXI] (Fig. 1D). All primers and probes were synthesized based on the NCBI reference SLC25A13 gene sequence (GenBank accession no. **NM_014251**) with the exception of mutation [XIX]:IVS16ins3kb, which was designed according to [19].

Real-time PCR and subsequent melting curve analyses were performed in a closed tube using a 20-μL mixture on a LightCycler 1.5 (Roche Diagnostics, Tokyo, Japan). The PCR mixture contained 2.0 μL of genomic DNA (10–50 ng), 0.5 μM of forward primer, 0.5 or 0.1 μM of reverse primer, 0.2 μM of each sensor and anchor probe, and 10 μL of Premix ExTaq™ (Perfect Real Time) reagent (TaKaRa Bio Inc., Otsu, Japan).

The thermal profile conditions were identical for all seven assays and consisted of an initial denaturation step (30 s at 95 °C), followed by 45 amplification cycles with the following conditions: denaturation for 5 s at 95 °C and annealing and extension for 20 s at 60 °C. The transition rate between all steps was 20 °C/s. After amplification, the samples were held at 37 °C for 1 min, followed by the melting curve acquisition at a ramp rate of 0.15 °C/s extending to 80 °C with continuous fluorescence acquisition.

Table 2
Primers, probes and target amplicon sequences, target mutation sites, and primer concentrations.

Primer/probe set	Name	Sequences of PCR products, primer locations, probe sequences, and mutation sites (5′ to 3′)	Concentration (μmol/L)
A		GGCTATACTGAAATATGAGAAatgaaaaaagggatgtttttaaattttataatgtaaattgtaataaattggtatatttgttgcttgtgtttgtttttcccctacagac	
		gtatgaccttagcagacattgaacggattgctcctctggaagagggaactctgccCTTTAACTTGGCTGAGG (181 bp)	
	Mut1-F	GGCTATACTGAAATATGAGAA	0.5
	Mut1-R	CCTCAGCCAAGTTAAAG	0.5
	Mut1-UP	ATGTAAATTGTAATAAATTGGTATATTTGTTGCTTGTGTT-FITC	
	Mut1-DW	LC Red640-GTTTTTCCCCTACAGAC**GACC**-P	
B		GAATGCAGAACCAACGAtcaactggctcttttgtgggagaactcatgtataaaaacagctttgactgttttaagaaagtgctacgctatgaaggcttctt	
		tggactgtatagaggttagtgccacatgctcaatacctgttaggtgaaataacactcaaaggtttggtttctcatcttagtgcctGACATGAATTAGCAAGACTG (205 bp)	
	Mut2-F	GAATGCAGAACCAACGA	0.5
	Mut2-R	CAGTCTTGCTAATTCATGTC	0.1
	Mut2-UP	ACCTAACAGGTATTGAGCATGTG-FITC	
	MUt2-DW	LC Red640-CACTAA**CC**TCTATACAGTCCA-P	
C		GCAGTTCAAAGCACAGTTATTtttatatagtgagaatgtgaccagactgagatggtgttgtgtctctcctgcaggtatgcctgcagcatctttagtg	
		accctgctgatgttatcaagacgagattacaggtg	
		gctgcccggg(**gagatta**caggtggctgcccggg)ctggccaaaccaCTTACAGCGGAGTGATAGAC (175 bp)	
	Mut3-F	GCAGTTCAAAGCACAGTTATT	0.5
	Mut3-R	GTCTATCACTCCGCTGTAAG	0.5
	Mut3-UP	ACCCCTGCTGATGTTATCAAGACGAGATTACAGGT-FITC	
	Mut3-DW	LC Red640-GCTGCCCGGG**GAGATTA**-P	
D		TCAATTTATTTGAGGCTGCtggaggtaccacatcccatcaagttagtttctcctattttaatggatttaattcgctccttaacaac	
		atggaactcattagaaagatctatagcactc	
		tggctggcaccaggaaagatgttgaagtGACTAAGGGTGAGTGAGAA (164 bp)	
	Mut4-F	TCAATTTATTTGAGGCTGC	0.5
	Mut4-R	TTCTCACTCACCCTTAGTC	0.5
	Mut4-UP	AATGGATTTAATT**C**GCTCCTTAACA-FITC	
	Mut4-DW	LC Red640-ATGGAACTCATTAGAAAGATCTATAGCACTC-P	
E		TGCACAAAGATGGTTCGgtcccacttgcagcagaaattcttgctggaggctgc**g**taagtacctttttgaagctctcttcattgaaaagacttgtttcac	
		atatatatcactaccatggtcaacaggtgtggactaaggcttctgttTAACCACAGATCCTGCA (162 bp)	
	Mut5-F	TGCACAAAGATGGTTCG	0.5
	Mut5-R	TGCAGGATCTGTGGTTA	0.5
	Mut5-UP	GTGAAACAAGTCTTTTCAATGAAGAGAGCTTC-FITC	
	Mut5-DW	LC Red640-AAGGTACTTA**C**GCAGCCTC-P	
F	normal allele	GGAGCTGGTGGTATGGAAataatgtgttcttaactaactctttggtatcaggtaaatttttaaaatatctaattatatctgtgatttctc	
		catttttttaaagctcgtgtatttcgatcctcaccccagtttggt	
		gtaactttgctgacttacgaattgctacagcgatggttctacattgattttggaggagtgtaagtatcatgctaaatctgctgctaaatttt	
		GGCTGCTGCTAATGCTC (244 bp)	
	insertion allele	CCATCTTCCTCCTCCCTTggcagccccgccccccgatttctccatttttttaaagctcgtgtatttcgatcctcaccccagtttggt	
		gtaactttgctgacttacgaattgctacagcgatggttctacattgatttt	
		ggaggagtgtaagtatcatgctaaatctgctgctaaattttGGCTGCTGCTAATGCTC (196 bp)	
	Mut19-N-F	GGAGCTGGTGGTATGGAA	0.5
	Mut19-ins-F	CCATCTTCCTCCTCCCTT	0.5
	Mut19-R	GAGCATTAGCAGCAGCC	0.5
	Mut19-UP	ACCAAACTGGGGTGAGGATCGAAATACACGAGCTTTAAAAAAATG-FITC	
	Mut19-N-DW	LC Red640-AGAAATCACAGATATAATTAGATATTT-P	
	Mut19-ins-DW	LC Red640-AGAAATCGGGGGGCGGGG-P	
G		TCTTAACTAACTCTTTGGTATCAGGTaaatttttaaaatatctaattatatctgtgatttctccatttttttaaagctcg	
		tgtatttcgatcctcaccccagtttggtgtaactttgc**t**gactt**a(a)cg**aattgctacag**c**ga	
		tggttctacattgatttttggaggagtgtaagtatcatgctaaatctgctgctaaattttGGCTGCTGCTAATGCTC (217 bp)	
	Mut6-9, 21-F	TCTTAACTAACTCTTTGGTATCAGGT	0.5
	Mut6-9, 21-R	GAGCATTAGCAGCAGCC	0.5
	Mut6-9, 21-UP	TGTATTTCGATCCTCACCCCAGTTTGGTGTAACTT-FITC	
	Mut6-9, 21-DW	LC Red640-GC**G**GACTT**ACG**AATTGCTACAG**C**GA-P	

Upper case and underlined letters indicate the locations of primers and probes, respectively. Inserted DNA is shown in parenthesis. Nucleotides in boldface were used for mutation detection.
F: forward, R: reverse, UP: upstream, DW: downstream, N: normal allele, ins: insertion allele, FITC: fluorescein isothiocyanate, P: phosphate.

Please cite this article as: A. Kikuchi, et al., Simple and rapid genetic testing for citrin deficiency by screening 11 prevalent mutations in *SLC25A13*, Mol. Genet. Metab. (2012), doi:10.1016/j.ymgme.2011.12.024

ARTICLE IN PRESS

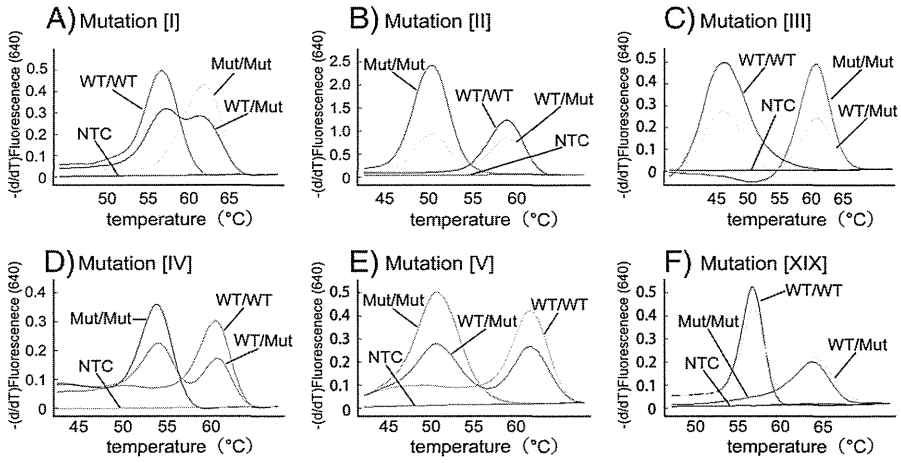

Fig. 2. Typical melting curves used in the detection of mutations [I–V] and [XIX]. Each assay using primer/probe sets A–F is displayed in a separate graph (A–F). WT: wild-type allele, Mut: mutant allele, NTC: no DNA template control.

2.3. Validation of the mutation detection system

After establishing the protocol for detecting the 11 prevalent mutations, 50 DNA samples from patients' blood were sent from Kagoshima University to Tohoku University for the validation of this system in a single-blind manner. Similarly, 26 DNA samples purified from paper-filter blood samples were analyzed in the same manner as the blood DNA samples.

2.4. Estimation of the carrier frequency

For the estimation of the heterozygous carrier frequency, 420 genomic DNA samples from healthy volunteers were screened using the HybProbe analysis for the 11 prevalent mutations. All detected mutations were confirmed by direct sequencing.

2.5. Ethics

This study was approved by the Ethical Committees of Tohoku University School of Medicine and Kagoshima University. Written informed consent was obtained from all participants or their guardians.

3. Results

3.1. Development of the mutation detection system

In primer/probe sets B, D, and E, the reporter probes were designed to be complimentary to the wild-type allele (Fig. 1A). To allow for an improved detection of the mutations, primer/probe sets A and C were designed to be complementary to the mutant allele (Figs. 1B, C). In the primer/probe set F, two forward PCR primers, which were specific to the wild-type and the mutant alleles, were used with a common reverse primer for the co-amplification of the wild-type and 3-kb insertion alleles (Fig. 1E). Two reporter probes, which had a common anchor probe, were used for the detection of the wild-type and mutant alleles. Because the two reporter probes had different melting temperatures, we were able to identify the allele that was amplified. Fig. 2 shows representative results of the melting curve analyses using the primer/probe sets A–F, in which all of the mutant alleles generated distinct peaks corresponding to the wild-type alleles.

In the primer/probe set G, we used a reporter probe that was complementary to the mutant [XXI] allele (Fig. 1D). All five mutations in exon 17 were successfully differentiated from the wild-type allele (Figs. 3A–E). The [XXIX] mutation is an additional mutation in exon

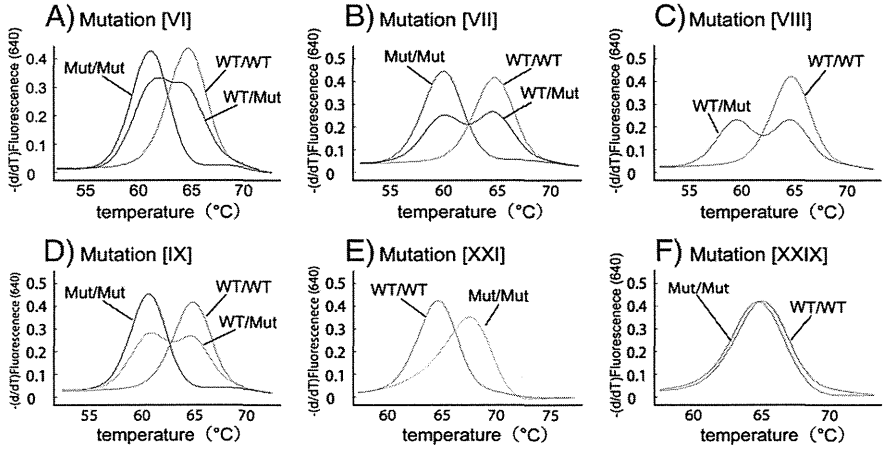

Fig. 3. Typical melting curves used in the detection of mutations [VI–XI], [XXI], and [XXIX] on exon 17. Genotyping was performed using primer/probe set G. Each melting curve for a target mutation is displayed in a separate graph (A–F). Note that mutation [XXIX] (F) is a non-target mutation on the anchor probe. WT: wild-type allele, Mut: mutant allele.

Please cite this article as: A. Kikuchi, et al., Simple and rapid genetic testing for citrin deficiency by screening 11 prevalent mutations in *SLC25A13*, Mol. Genet. Metab. (2012), doi:10.1016/j.ymgme.2011.12.024

17 that is not listed in Table 1. The [XXIX] mutation is located in the anchor-probe binding site and not on the reporter-probe binding site (Fig. 1D). To examine the effect of mutations on the anchor probe, we genotyped a patient with a heterozygous [XXIX] mutation using primer/probe set G (Fig. 3F). We found no change in the melting curves between the wild-type allele and the [XXIX] allele, thereby suggesting that point mutations within the anchor probe sequence have little effect on the melting curve analysis.

3.2. Validation

The genotypes determined at Tohoku University using the proposed method and those determined at Kagoshima University using a previously published method were identical for the 11 common mutations (Table S1 in supplementary material). We performed a similar test using DNA samples purified from filter-paper blood samples to determine if this method could be used for newborn screening. The genotypes determined in both laboratories were identical for all 26 DNA samples (Table S2 in supplementary material).

3.3. Frequency of eleven prevalent mutations

We found four heterozygous carriers of mutation [I], three of mutation [II], and two of mutation [V]. In addition, primer/probe set G detected one heterozygous mutation, which was confirmed as mutation [VIII] by direct sequencing. Altogether, 10 mutations were detected in 420 Japanese healthy controls.

4. Discussion

We developed a simple and rapid genetic test using real-time PCR combined with the HybProbe system for the 11 prevalent mutations in *SLC25A13*: mutations [I], [II], [III], [IV], [V], [VI], [VII], [VIII], [IX], [XIX], and [XXI]. This genetic test is a closed-tube assay in which no post-PCR handling of the samples is required. In addition, the genotyping is completed within 1 h. This test can utilize DNA samples purified from both peripheral blood and filter-paper blood. The reliability of the test was confirmed by genotyping 76 blind DNA samples from patients with citrin deficiency, including 50 peripheral blood and 26 filter-paper blood DNA samples. Because screening for the 11 targeted mutations would identify 95% of mutant alleles in the Japanese population [19], both, one, and no mutant alleles are expected to be identified in 90.4%, 9.3%, and less than 0.3% of patients, respectively. This genetic test would be useful not only in Japan but also other East Asian countries, including China, Korea, Taiwan and Vietnam, in which the same mutations are prevalent. Our test is expected to detect 76–87% of the mutant alleles in the Chinese population [12,19,25], 95–100% in the Korean population [12,19,26], 60–68% in the Taiwanese population [27,28], and 100% in the Vietnamese population [12,19]. If we were to prepare a primer/probe set for mutation [X]:g.IVS6+5G>A [12], which is prevalent in Taiwan, the estimated sensitivity would exceed 90% in the Taiwanese population [27,28].

Recently, the high resolution melting (HRM) method was reported to be suitable for the screening of mutations in the diagnosis of citrin deficiency [28]. HRM analysis is a closed-tube assay that screens for any base changes in the amplicons. The presence of SNPs anywhere on the amplicons can affect the melting curve, thereby suggesting that HRM is not suitable for screening for known mutations, but rather, is best suited to screening for unknown mutations. When we detected one heterozygous prevalent mutation, we performed HRM screening for all 17 exons of *SLC25A13*. After HRM screening, only the HRM-positive exons were subjected to direct sequencing analysis. Several mutant alleles were identified using this approach.

The frequency of homozygotes, including compound heterozygotes, presenting *SLC25A13* mutations in the population at Kagoshima (a prefecture in the southern part of Japan) has been calculated to be 1/17,000 based on the carrier rate (1/65) [19]. The prevalence of NICCD has been also reported to be 1/17,000–34,000 [29]. In this study, the carrier rate in Miyagi (a prefecture in northern Japan) was 1/42 (95% confidential interval, 1/108–1/26), thereby yielding an estimated frequency of patients with citrin deficiency of 1/7,100. Our result, together with the previous report [19], suggests that a substantial fraction of the homozygotes or compound heterozygotes of SLC25A13 mutations was asymptomatic during the neonatal period.

The early and definitive diagnosis of citrin deficiency may be beneficial for patients with citrin deficiency by encouraging specific dietary habits and avoiding iatrogenic worsening of brain edema by glycerol infusion when patients develop encephalopathy [30,31]. Because the screening of blood citrulline levels by tandem mass analysis at birth does not detect all patients with citrin deficiency, the development of a genetic test would be welcomed. In this study, we demonstrated that genomic DNA extracted from filter paper blood samples was correctly genotyped, thereby indicating the feasibility of newborn screening using this genetic test. If 100,000 babies in the northern part of Japan were screened by this method, we would detect 14 homozygotes or compound heterozygotes with *SLC25A13* mutations and 2400 heterozygous carriers. In 2400 heterozygous carriers, we would expect to observe only 1 to 2 compound heterozygotes with one target and one non-target mutation. The estimated frequency of babies with two non-target mutations is 0.04/100,000. Our genetic method would therefore allow us to screen newborn babies efficiently. If we performed this genetic test in a high-throughput real-time PCR system, such as a 384- or 1,536-well format, the cost per sample could be lowered.

In conclusion, we have established a rapid and simple detection system using the HybProbe assay for the 11 prevalent mutations in *SLC25A13*. This system could be used to screen newborns for citrin deficiency and may facilitate the genetic diagnosis of citrin deficiency, especially in East Asian populations.

Supplementary materials related to this article can be found online at doi:10.1016/j.ymgme.2011.12.024.

Acknowledgments

The authors acknowledge the contribution of Dr. Keiko Kobayashi, who passed away on December 21th, 2010. Dr. Kobayashi discovered that the *SLC25A13* gene is responsible for citrin deficiency and devoted much of her life to elucidating the mechanism of citrin deficiency. This work was supported by grants from the Ministry of Education, Culture, Sports, Science, and Technology and the Ministry of Health, Labor, and Public Welfare.

References

[1] K. Kobayashi, D.S. Sinasac, M. Iijima, A.P. Boright, L. Begum, J.R. Lee, T. Yasuda, S. Ikeda, R. Hirano, H. Terazono, M.A. Crackower, I. Kondo, L.C. Tsui, S.W. Scherer, T. Saheki, The gene mutated in adult-onset type II citrullinaemia encodes a putative mitochondrial carrier protein, Nat. Genet. 22 (1999) 159–163.
[2] T. Ohura, K. Kobayashi, Y. Tazawa, I. Nishi, D. Abukawa, O. Sakamoto, K. Iinuma, T. Saheki, Neonatal presentation of adult-onset type II citrullinemia, Hum. Genet. 108 (2001) 87–90.
[3] Y. Tazawa, K. Kobayashi, T. Ohura, D. Abukawa, F. Nishinomiya, Y. Hosoda, M. Yamashita, I. Nagata, Y. Kono, T. Yasuda, N. Yamaguchi, T. Saheki, Infantile cholestatic jaundice associated with adult-onset type II citrullinemia, J. Pediatr. 138 (2001) 735–740.
[4] T. Tomomasa, K. Kobayashi, H. Kaneko, H. Shimura, T. Fukusato, M. Tabata, Y. Inoue, S. Ohwada, M. Kasahara, Y. Morishita, M. Kimura, T. Saheki, A. Morikawa, Possible clinical and histologic manifestations of adult-onset type II citrullinemia in early infancy, J. Pediatr. 138 (2001) 741–743.
[5] T. Shigeta, M. Kasahara, T. Kimura, A. Fukuda, K. Sasaki, K. Arai, A. Nakagawa, S. Nakagawa, K. Kobayashi, S. Soneda, H. Kitagawa, Liver transplantation for an

ARTICLE IN PRESS

infant with neonatal intrahepatic cholestasis caused by citrin deficiency using heterozygote living donor, Pediatr. Transplant. 14 (2009) E86–88.
[6] M. Kasahara, S. Ohwada, T. Takeichi, H. Kaneko, T. Tomomasa, A. Morikawa, K. Yonemura, K. Asonuma, K. Tanaka, K. Kobayashi, T. Saheki, I. Takeyoshi, Y. Morishita, Living-related liver transplantation for type II citrullinemia using a graft from heterozygote donor, Transplantation 71 (2001) 157–159.
[7] Y. Takashima, M. Koide, H. Fukunaga, M. Iwai, M. Miura, R. Yoneda, T. Fukuda, K. Kobayashi, T. Saheki, Recovery from marked altered consciousness in a patient with adult-onset type II citrullinemia diagnosed by DNA analysis and treated with a living related partial liver transplantation, Intern. Med. 41 (2002) 555–560.
[8] A. Tamamori, Y. Okano, H. Ozaki, A. Fujimoto, M. Kajiwara, K. Fukuda, K. Kobayashi, T. Saheki, Y. Tagami, T. Yamano, Neonatal intrahepatic cholestasis caused by citrin deficiency: severe hepatic dysfunction in an infant requiring liver transplantation, Eur. J. Pediatr. 161 (2002) 609–613.
[9] T. Ohura, K. Kobayashi, Y. Tazawa, D. Abukawa, O. Sakamoto, S. Tsuchiya, T. Saheki, Clinical pictures of 75 patients with neonatal intrahepatic cholestasis caused by citrin deficiency (NICCD), J. Inherit. Metab. Dis. 30 (2007) 139–144.
[10] T. Yasuda, N. Yamaguchi, K. Kobayashi, I. Nishi, H. Horinouchi, M.A. Jalil, M.X. Li, M. Ushikai, M. Iijima, I. Kondo, T. Saheki, Identification of two novel mutations in the SLC25A13 gene and detection of seven mutations in 102 patients with adult-onset type II citrullinemia, Hum. Genet. 107 (2000) 537–545.
[11] N. Yamaguchi, K. Kobayashi, T. Yasuda, I. Nishi, M. Iijima, M. Nakagawa, M. Osame, I. Kondo, T. Saheki, Screening of SLC25A13 mutations in early and late onset patients with citrin deficiency and in the Japanese population: identification of two novel mutations and establishment of multiple DNA diagnosis methods for nine mutations, Hum. Mutat. 19 (2002) 122–130.
[12] Y.B. Lu, K. Kobayashi, M. Ushikai, A. Tabata, M. Iijima, M.X. Li, L. Lei, K. Kawabe, S. Taura, Y. Yang, T.-T. Liu, S.-H. Chiang, K.-J. Hsiao, Y.-L. Lau, L.-C. Tsui, D.H. Lee, T. Saheki, Frequency and distribution in East Asia of 12 mutations identified in the SLC25A13 gene of Japanese patients with citrin deficiency, J. Hum. Genet. 50 (2005) 338–346.
[13] E. Ben-Shalom, K. Kobayashi, A. Shaag, T. Yasuda, H.-Z. Gao, T. Saheki, C. Bachmann, O. Elpeleg, Infantile citrullinemia caused by citrin deficiency with increased dibasic amino acids, Mol. Genet. Metab. 77 (2002) 202–208.
[14] J. Takaya, K. Kobayashi, A. Ohashi, M. Ushikai, A. Tabata, S. Fujimoto, F. Yamato, T. Saheki, Y. Kobayashi, Variant clinical courses of 2 patients with neonatal intrahepatic cholestasis who have a novel mutation of SLC25A13, Metab. Clin. Exp. 54 (2005) 1615–1619.
[15] A. Luder, A. Tabata, M. Iijima, K. Kobayashi, H. Mandel, Citrullinaemia type 2 outside East Asia: Israeli experience, J. Inherit. Metab. Dis. 29 (2006) 59.
[16] T. Hutchin, M. Preece, K. Kobayashi, T. Saheki, R. Brown, D. Kelly, P. McKiernan, A. Green, U. Baumann, Neonatal intrahepatic cholestasis caused by citirn deficiency (NICCD) in a European patient, J. Inherit. Metab. Dis. 29 (2006) 112.
[17] J.-S. Sheng, M. Ushikai, M. Iijima, S. Packman, K. Weisiger, M. Martin, M. McCracken, T. Saheki, K. Kobayashi, Identification of a novel mutation in a Taiwanese patient with citrin deficiency, J. Inherit. Metab. Dis. 29 (2006) 163.
[18] J.M. Ko, G.-H. Kim, J.-H. Kim, J.Y. Kim, J.-H. Choi, M. Ushikai, T. Saheki, K. Kobayashi, H.-W. Yoo, Six cases of citrin deficiency in Korea, Int. J. Mol. Med. 20 (2007) 809–815.
[19] A. Tabata, J.-S. Sheng, M. Ushikai, Y.-Z. Song, H.-Z. Gao, Y.-B. Lu, F. Okumura, M. Iijima, K. Mutoh, S. Kishida, T. Saheki, K. Kobayashi, Identification of 13 novel mutations including a retrotransposal insertion in SLC25A13 gene and frequency of 30 mutations found in patients with citrin deficiency, J. Hum. Genet. 53 (2008) 534–545.
[20] P.S. Bernard, R.S. Ajioka, J.P. Kushner, C.T. Wittwer, Homogeneous multiplex genotyping of hemochromatosis mutations with fluorescent hybridization probes, Am. J. Pathol. 153 (1998) 1055–1061.
[21] C.N. Gundry, P.S. Bernard, M.G. Herrmann, G.H. Reed, C.T. Wittwer, Rapid F508del and F508C assay using fluorescent hybridization probes, Genet. Test. 3 (1999) 365–370.
[22] T. Saheki, K. Kobayashi, I. Inoue, Hereditary disorders of the urea cycle in man: biochemical and molecular approaches, Rev. Physiol. Biochem. Pharmacol. 108 (1987) 21–68.
[23] K. Kobayashi, M. Horiuchi, T. Saheki, Pancreatic secretory trypsin inhibitor as a diagnostic marker for adult-onset type II citrullinemia, Hepatology 25 (1997) 1160–1165.
[24] Y. Tazawa, K. Kobayashi, D. Abukawa, I. Nagata, S. Maisawa, R. Sumazaki, T. Iizuka, Y. Hosoda, M. Okamoto, J. Murakami, S. Kaji, A. Tabata, Y.B. Lu, O. Sakamoto, A. Matsui, S. Kanzaki, G. Takada, T. Saheki, K. Iinuma, T. Ohura, Clinical heterogeneity of neonatal intrahepatic cholestasis caused by citrin deficiency: case reports from 16 patients, Mol. Genet. Metab. 83 (2004) 213–219.
[25] H.Y. Fu, S.R. Zhang, X.H. Wang, T. Saheki, K. Kobayashi, J.S. Wang, The mutation spectrum of the SLC25A13 gene in Chinese infants with intrahepatic cholestasis and aminoacidemia, J. Gastroenterol. 46 (2011) 510–518.
[26] K. Kobayashi, Y.B. Lu, M.X. Li, I. Nishi, K.-J. Hsiao, K. Choeh, Y. Yang, W.-L. Hwu, J.K.V. Reichardt, F. Palmieri, Y. Okano, T. Saheki, Screening of nine SLC25A13 mutations: their frequency in patients with citrin deficiency and high carrier rates in Asian populations, Mol. Genet. Metab. 80 (2003) 356–359.
[27] T. Saheki, K. Kobayashi, M. Iijima, M. Horiuchi, L. Begum, M.A. Jalil, M.X. Li, Y.B. Lu, M. Ushikai, A. Tabata, M. Moriyama, K.-J. Hsiao, Y. Yang, Adult-onset type II citrullinemia and idiopathic neonatal hepatitis caused by citrin deficiency: involvement of the aspartate glutamate carrier for urea synthesis and maintenance of the urea cycle, Mol. Genet. Metab. 81 (Suppl 1) (2004) S20–S26.
[28] J.T. Lin, K.J. Hsiao, C.Y. Chen, C.C. Wu, S.J. Lin, Y.Y. Chou, S.C. Shiesh, High resolution melting analysis for the detection of SLC25A13 gene mutations in Taiwan, Clin. Chim. Acta 412 (2011) 460–465.
[29] Y. Shigematsu, S. Hirano, I. Hata, Y. Tanaka, M. Sudo, N. Sakura, T. Tajima, S. Yamaguchi, Newborn mass screening and selective screening using electrospray tandem mass spectrometry in Japan, J. Chromatogr. B Analyt. Technol. Biomed. Life Sci. 776 (2002) 39–48.
[30] M. Yazaki, Y.-i. Takei, K. Kobayashi, T. Saheki, S.-I. Ikeda, Risk of worsened encephalopathy after intravenous glycerol therapy in patients with adult-onset type II citrullinemia (CTLN2), Intern. Med. 44 (2005) 188–195.
[31] H. Takahashi, T. Kagawa, K. Kobayashi, H. Hirabayashi, M. Yui, L. Begum, T. Mine, S. Takagi, T. Saheki, Y. Shinohara, A case of adult-onset type II citrullinemia—deterioration of clinical course after infusion of hyperosmotic and high sugar solutions, Med. Sci. Monit. 12 (2006) CS13–CS15.

Please cite this article as: A. Kikuchi, et al., Simple and rapid genetic testing for citrin deficiency by screening 11 prevalent mutations in *SLC25A13*, Mol. Genet. Metab. (2012), doi:10.1016/j.ymgme.2011.12.024

Neurology®

Clinical Reasoning: A young man with progressive subcortical lesions and optic nerve atrophy

Shoko Komatsuzaki, Osamu Sakamoto, Nobuo Fuse, et al.

Neurology 2012;79;e63
DOI 10.1212/WNL.0b013e3182648bb6

This information is current as of February 28, 2013

The online version of this article, along with updated information and services, is located on the World Wide Web at:
http://www.neurology.org/content/79/7/e63.full.html

Neurology ® is the official journal of the American Academy of Neurology. Published continuously since 1951, it is now a weekly with 48 issues per year. Copyright © 2012 American Academy of Neurology. All rights reserved. Print ISSN: 0028-3878. Online ISSN: 1526-632X.

AMERICAN ACADEMY OF NEUROLOGY®

RESIDENT & FELLOW SECTION

Section Editor
Mitchell S.V. Elkind, MD, MS

Clinical Reasoning: A young man with progressive subcortical lesions and optic nerve atrophy

Shoko Komatsuzaki, MD, PhD
Osamu Sakamoto, MD, PhD
Nobuo Fuse, MD, PhD
Mitsugu Uematsu, MD, PhD
Yoichi Matsubara, MD
Toshihiro Ohura, MD, PhD

Correspondence & reprint requests to Dr. Komatsuzaki: komatsuzaki@med.tohoku.ac.jp

SECTION 1

The male patient is the third child of unrelated Japanese parents. His older sister had tachypnea and feeding difficulties, and died at 5 days of age. The patient was delivered at term (birthweight, 3.8 kg), following an unremarkable pregnancy. He presented with tachypnea, metabolic acidosis, and hyperammonemia (944 μmol · L^{-1}) at 6 days.

Questions for consideration:

1. What is the differential for infantile presentation of hyperammonemia in the neonatal period?
2. What laboratory tests would you pursue?

GO TO SECTION 2

From the Departments of Medical Genetics (S.K., Y.M.) and Pediatrics (O.S., M.U., T.O.), Tohoku University School of Medicine, Sendai; Department of Ophthalmology (N.F.), Tohoku University Graduate School of Medicine, Sendai; and Department of Pediatrics (T.O.), Sendai City Hospital, Sendai, Japan.

Go to Neurology.org for full disclosures. Disclosures deemed relevant by the authors, if any, are provided at the end of this article.

Copyright © 2012 by AAN Enterprises, Inc.

Copyright © by AAN Enterprises, Inc. Unauthorized reproduction of this article is prohibited.

SECTION 2

Hyperammonemia occurs in urea cycle disorders (e.g., ornithine transcarbamylase deficiency) and organic acidurias (e.g., methylmalonic aciduria, propionic aciduria, and isovaleric aciduria) and fatty acid oxidation defects (e.g., multiple acyl-CoA dehydrogenase deficiency). The existence of acidosis with ketosis indicates organic aciduria, whereas respiratory alkalosis is observed in urea cycle defects. Diagnosis is based on quantitative assay of amino acids and acylcarnitines from dried blood and organic acids in urine samples.

Case: part 2. Elevated levels of 2-methylcitric acid and 3-hydroxypropionic acid were found in the urine. The plasma propionic acid concentration was increased (4.5 $mg \cdot dL^{-1}$), and propionyl-CoA carboxylase (PCC) activity in fibroblasts was decreased (6.3 $pmol \cdot min^{-1} \cdot mg^{-1}$ protein, normal value: 292 [n = 4]). The patient was treated with exchange transfusion, peritoneal dialysis, high-calorie infusions, and a low-protein diet.

Questions for consideration:

1. What is the diagnosis?
2. How should these infants be treated in the acute period?
3. What treatment should be given long term?

GO TO SECTION 3

Copyright © by AAN Enterprises, Inc. Unauthorized reproduction of this article is prohibited.

Propionic aciduria is an autosomal recessive disease caused by a deficiency of PCC. PCC is a biotin-dependent enzyme that catalyzes the branched chain amino acids valine and isoleucine but not leucine; it also catalyzes methionine, threonine, and odd-chain fatty acids in the mitochondrial matrix. PCC is composed of α and β subunits, which are encoded by nuclear genes *PCCA* and *PCCB*, respectively. PCC deficiency causes accumulation of propionic acid, 3-hydroxypropionic acid, 2-methylcitric acid, and propionylglycine in blood, urine, and CSF.[1]

Clinical forms of propionic aciduria are described on the basis of the age at onset: neonatal and late onset. The neonatal-onset form is characterized by poor sucking, vomiting, failure to thrive, and progressive encephalopathy. Routine laboratory findings are metabolic acidosis, ketosis, lactic acidosis, hyperammonemia, leukocytopenia, thrombocytopenia, and anemia. The late-onset form is characterized by periodic vomiting to life-threatening hyperammonemia, psychomotor retardation, and other chronic symptoms.[1] Propionic aciduria is characterized by increased excretion of propionic acid, 3-hydroxy propionic acid, and 2-methylcitric acid in urine as well as elevated concentrations of propionyl-carnitine in blood serum or plasma. It is initially diagnosed based on enzymatic analysis of propionyl-CoA carboxylase activity in fibroblasts or leukocytes. Identification of the specific mutations in *PCCA* or *PCCB* is required to confirm the diagnosis.[1]

The increased 2-methylcitric acid and 3-hydroxypropionic acid levels and decreased propionyl-CoA carboxylase activity in this case indicated propionic aciduria. Mutation analysis revealed homozygosity for p.Thr428Ile in the *PCCB* gene, confirming propionic aciduria.

Emergency treatment for propionic aciduria involves low-protein, high-energy nutrition and rehydration. Almost all propionic aciduria patients show hyperammonemia, which results from inhibition of urea cycle enzymes by accumulated acyl-CoA esters. Some patients, especially those severely affected, require hemodialysis/hemofiltration. Sodium benzoate and carbamyl glutamate are used to treat secondary hyperammonemia.[2] Long-term management comprises low-protein diet and carnitine supplementation. Arginine and carnitine are administered for detoxification of toxic metabolites. Metronidazole is often administered to reduce production of propionic acid by gut bacteria.[1]

Case: part 3. After emergency intervention, the patient was treated with a low-protein diet and carnitine supplementation. During the first 5 years of life, he had several episodes of metabolic acidosis requiring hospitalization; however, he never showed metabolic decompensation thereafter. Despite nearly normal development at 4 years, he thereafter developed intellectual deficits that gradually deteriorated with age: his developmental quotient was 88 at the age of 4 and 74 at 6, while his IQ was 73 at the age of 7 and 54 at 15.

At 22 years, metronidazole administration was initiated to reduce propionic acid production by gut bacteria. Bilateral vision impairment was also detected during a regular health check-up. Ophthalmologic examination showed temporal pallor of the right eye and left optic nerve atrophy (figure 1). The patient's visual acuity was 20/200 in the right eye and 20/300 in the left eye. In both eyes, his visual fields showed central scotoma, and his visual evoked potential (VEP) displayed decreased amplitude. An electroretinogram showed normal findings, while optical coherence tomography revealed no retinal structure abnormalities. Within a year, his visual acuity decreased from 20/200 to hand motion in the right eye and from 20/300 to counting fingers in the left. He also had intention tremor, mild hyperammonemia, and elevated lactic acid levels, but no metabolic acidosis. Ophthalmologic examination results at 11 years were normal.

Brain MRI revealed symmetric lesions of the basal ganglia, including the caudate nucleus, putamen, and globus pallidus (figure 2A). At 23 years, no symptoms were present, but diffusion-weighted MRI of the brain showed subcortical lesions (figure 2, B–D). At 24 years, he showed acute reversible muscle weakness and dysarthria, comparable to pseudobulbar paralysis. Neurologic evaluation showed increased deep tendon reflexes on the left side of the body, while subsequent MRI of the brain revealed progression of the subcortical lesions (figure 2, E–G), without evidence of metabolic decompensation.

Figure 1 **Fundal images**

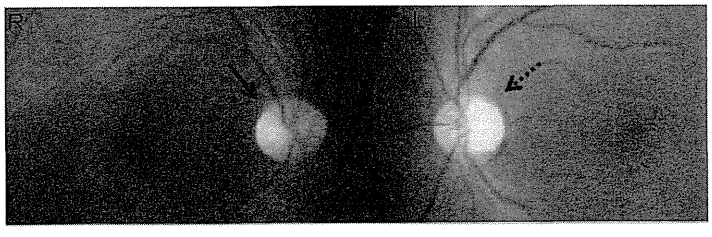

Temporal pallor in the right eye and optic nerve atrophy in the left.

Copyright © by AAN Enterprises, Inc. Unauthorized reproduction of this article is prohibited.

Figure 2 MRI

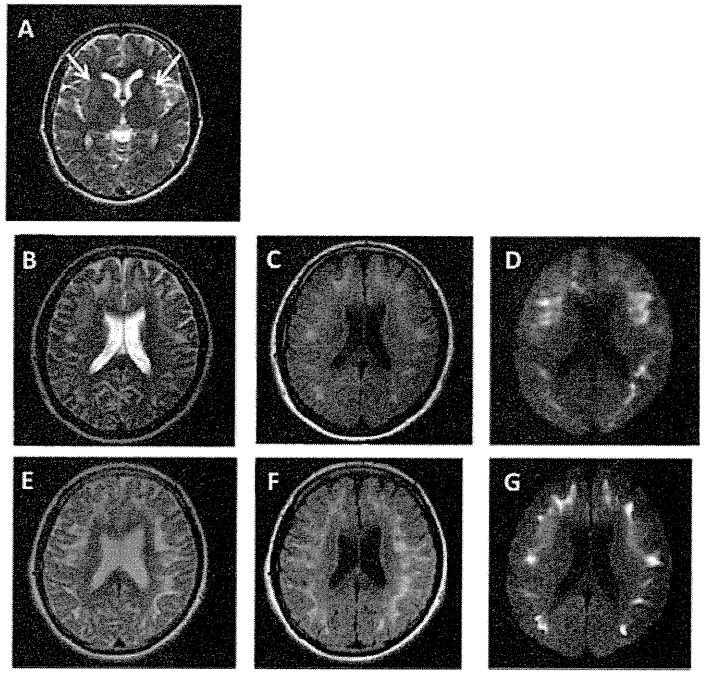

(A, B, E) T2-weighted images; the arrows in A indicate the high intensity of basal ganglia areas. (C, F) Fluid-attenuated inversion recovery. (D, G) Diffusion-weighted imaging, showing abnormal signals in subcortical lesions.

At 24 years, chest radiography showed an increased cardiothoracic ratio (65%) and pulmonary edema. Echocardiogram showed dilated hypokinetic left ventricle and a decrease in ejection fraction (48%), resembling dilated cardiomyopathy. The patient was administered furosemide, spironolactone, and carvedilol.

Questions for consideration:

1. Why did this patient's condition deteriorate even without metabolic acidosis crises?
2. What is the range of prognosis for neonatal-onset form propionic aciduria?
3. What type of monitoring will he need?

GO TO SECTION 4

Copyright © by AAN Enterprises, Inc. Unauthorized reproduction of this article is prohibited.

SECTION 4

The accumulation of toxic organic acids causes cerebral stroke that cannot be accounted for by hypoxemia or vascular insufficiency: this neurologic event is termed metabolic stroke.[3] Toxic metabolites cause secondary mitochondrial dysfunction, which leads to metabolic stroke.[4] According to the recent "trapping hypothesis," the limited transport of toxic metabolites from the brain to the blood compartment leads to accumulation of toxic dicarboxylic acids in glutaric aciduria type I and methylmalonic aciduria.[5] Like propionic aciduria, methylmalonic aciduria is also a branched-chain amino acid disorder. For propionic aciduria patients, accumulation of the dicarboxylic acid 2-methylcitric acid seems likely; however, it has not yet been sufficiently documented.

Patients with propionic aciduria and methylmalonic aciduria often present with mental retardation, epilepsy, and extrapyramidal symptoms. Sixty percent of patients with propionic aciduria have an IQ lower than 75.[2] Symmetric lesions of the basal ganglia are the most frequently reported MRI changes in propionic aciduria and methylmalonic aciduria.[2] Subcortical white matter abnormality was additionally reported in 11.5% of patients with methylmalonic aciduria.[6] However, these findings have not been confirmed in propionic aciduria, probably because the number of patients is relatively small.

Compared to previously reported late-onset optic nerve atrophy in patients with methylmalonic aciduria and propionic aciduria,[7] our patient is the oldest. The previous report suggested that optic nerve atrophy observed in propionic aciduria and methylmalonic aciduria resembled Leber hereditary optic neuropathy (LHON),[7] as both showed optic nerve atrophy and normal retina. LHON is caused by 1 of 3 pathogenic mtDNA mutations at the nucleotide positions 11,778, 3,460, and 14,484, located in genes encoding the mitochondrial complex I subunits. Our patient carried none of these mutations. The common findings between optic nerve atrophy in propionic aciduria/methylmalonic aciduria and LHON suggest that secondary mitochondrial dysfunction leads to optic nerve atrophy in patients with propionic aciduria and methylmalonic aciduria. Optic nerve atrophy is age-dependent, but independent of metabolic control, other neurologic complications, and overall health status.[7] Therefore, we recommend regular ophthalmologic examination of patients with propionica aciduria and methylmalonic aciduria.

In many countries, propionic aciduria is targeted in newborn screening programs. About 60% of patients diagnosed through newborn screening were already symptomatic and less than 10% remained asymptomatic.[8] Even though newborn screening diagnosis does not positively correlate with a milder clinical course or better neurologic outcome,[8] it is important from the viewpoint of earlier diagnosis and decreased early mortality.

According to genotype and phenotype correlation analysis, certain null mutations are related to neonatal onset, while certain missense mutations are related to the late-onset form.[9] Although late-onset patients have higher survival rates compared to neonatal-onset patients,[9] both face the risk of relapses of life-threatening episodes of metabolic decompensation and risk of death or further neurologic damage.

PCC plays a role mainly in the liver; therefore, liver transplantation has been considered an alternative therapy.[2] Liver transplantation minimizes further metabolic acidosis and improves the quality of life. However, various complications, including basal ganglia lesions, cardiomyopathy, and optic nerve atrophy, were reported in patients without metabolic decompensation.[2,7] Even after liver transplantation, stroke-like episodes or cardiomyopathy was reported.[10]

Thus, conventional management is insufficient to improve the long-term prognosis for propionic aciduria patients, indicating the need for novel therapeutic approaches based on a better understanding of the pathophysiology.

AUTHOR CONTRIBUTIONS

Shoko Komatsuzaki contributed to conceptualizing the study and design, analysis and interpretation of data, drafting/revising the manuscript. Osamu Sakamoto contributed to the analysis and interpretation of the data, drafting/revising the manuscript. Nobuo Fuse contributed to the analysis and interpretation of data, drafting/revising the manuscript. Mitsugu Uematsu contributed to the analysis and interpretation of data, drafting/revising the manuscript. Yoichi Matsubara contributed to drafting/revising the manuscript. Toshihiro Ohura contributed in critical review of the manuscript, reviewed the literature for manuscript preparation, and supervised the clinical management of study patients.

ACKNOWLEDGMENT

The authors thank Professor Shigeo Kure and Dr. Shuhei Kakizaki at the Department of Pediatrics, Tohoku University, for collection of the patients' clinical data and comments on the manuscript; and Professor Stefan Koelker and Dr. Sven Sauer at Children's Hospital Heidelberg for their comments on the manuscript.

DISCLOSURE

The authors report no disclosures relevant to the manuscript. **Go to Neurology.org for full disclosures.**

REFERENCES

1. Fenton WA, Gravel RA, Rosenblatt DS. Disorders of propionate and methylmalonate metabolism. In: Scrver CR, Beaudet AL, Sly WS, Valle D, eds. The Metabolic and Molecular Bases of Inherited Metabolic Disease. New York: McGraw-Hill; 2001:2165–2193.
2. de Baulny HO, Benoist JF, Rigal O, Touati G, Rabier D, Saudubray JM. Methylmalonic and propionic acidaemias: management and outcome. J Inherit Metab Dis 2005;28: 415–423.

Copyright © by AAN Enterprises, Inc. Unauthorized reproduction of this article is prohibited.

3. Heidenreich R, Natowicz M, Hainline BE, et al. Acute extrapyramidal syndrome in methylmalonic acidemia: "metabolic stroke" involving the globus pallidus. J Pediatr 1988;113:1022–1027.
4. Schwab MA, Sauer SW, Okun JG, et al. Secondary mitochondrial dysfunction in propionic aciduria: a pathogenic role for endogenous mitochondrial toxins. Biochem J 2006;398:107–112.
5. Sauer SW, Opp S, Mahringer A, et al. Glutaric aciduria type I and methylmalonic aciduria: simulation of cerebral import and export of accumulating neurotoxic dicarboxylic acids in in vitro models of the blood-brain barrier and the choroid plexus. Biochim Biophys Acta 2010;1802:552–560.
6. Radmanesh A, Zaman T, Ghanaati H, Molaei S, Robertson RL, Zamani AA. Methylmalonic acidemia: brain imaging findings in 52 children and a review of the literature. Pediatr Radiol 2008;38:1054–1061.
7. Williams ZR, Hurley PE, Altiparmak UE, et al. Late onset optic neuropathy in methylmalonic and propionic acidemia. Am J Ophthalmol 2009;147:929–933.
8. Grunert SC, Mullerleile S, de Silva L, et al. Propionic acidemia: neonatal versus selective metabolic screening. J Inherit Metab Dis 2012;35:41–49.
9. Perez-Cerda C, Merinero B, Rodriguez-Pombo P, et al. Potential relationship between genotype and clinical outcome in propionic acidaemia patients. Eur J Hum Genet 2000;8:187–194.
10. Collins J, Kelly D. Cardiomyopathy in propionic acidemia. Eur J Pediatr 1994;153:53.

Copyright © by AAN Enterprises, Inc. Unauthorized reproduction of this article is prohibited.

Clinical Reasoning: A young man with progressive subcortical lesions and optic nerve atrophy

Shoko Komatsuzaki, Osamu Sakamoto, Nobuo Fuse, et al.

Neurology 2012;79;e63
DOI 10.1212/WNL.0b013e3182648bb6

This information is current as of February 28, 2013

Updated Information & Services	including high resolution figures, can be found at: http://www.neurology.org/content/79/7/e63.full.html
Subspecialty Collections	This article, along with others on similar topics, appears in the following collection(s): **All Pediatric** http://www.neurology.org/cgi/collection/all_pediatric **Metabolic disease (inherited)** http://www.neurology.org/cgi/collection/metabolic_disease_inherited **Optic nerve** http://www.neurology.org/cgi/collection/optic_nerve **Organic acid** http://www.neurology.org/cgi/collection/organic_acid
Permissions & Licensing	Information about reproducing this article in parts (figures, tables) or in its entirety can be found online at: http://www.neurology.org/misc/about.xhtml#permissions
Reprints	Information about ordering reprints can be found online: http://www.neurology.org/misc/addir.xhtml#reprintsus

AMERICAN ACADEMY OF NEUROLOGY®

Homozygous c.14576G>A variant of *RNF213* predicts early-onset and severe form of moyamoya disease

S. Miyatake, MD
N. Miyake, MD, PhD
H. Touho, MD, PhD
A. Nishimura-Tadaki, PhD
Y. Kondo, MD
I. Okada, MD
Y. Tsurusaki, PhD
H. Doi, MD, PhD
H. Sakai, PhD
H. Saitsu, MD, PhD
K. Shimojima, MD
T. Yamamoto, MD, PhD
M. Higurashi, MD
N. Kawahara, MD, PhD
H. Kawauchi, MD
K. Nagasaka, MD, PhD
N. Okamoto, MD
T. Mori, MD, PhD
S. Koyano, MD, PhD
Y. Kuroiwa, MD, PhD
M. Taguri, PhD
S. Morita, PhD
Y. Matsubara, MD, PhD
S. Kure, MD, PhD
N. Matsumoto, MD, PhD

Correspondence & reprint requests to Dr. Matsumoto: naomat@yokohama-cu.ac.jp

ABSTRACT

Objective: *RNF213* was recently reported as a susceptibility gene for moyamoya disease (MMD). Our aim was to clarify the correlation between the *RNF213* genotype and MMD phenotype.

Methods: The entire coding region of the *RNF213* gene was sequenced in 204 patients with MMD, and corresponding variants were checked in 62 pairs of parents, 13 mothers and 4 fathers of the patients, and 283 normal controls. Clinical information was collected. Genotype-phenotype correlations were statistically analyzed.

Results: The c.14576G>A variant was identified in 95.1% of patients with familial MMD, 79.2% of patients with sporadic MMD, and 1.8% of controls, thus confirming its association with MMD, with an odds ratio of 259 and $p < 0.001$ for either heterozygotes or homozygotes. Homozygous c.14576G>A was observed in 15 patients but not in the controls and unaffected parents. The incidence rate for homozygotes was calculated to be >78%. Homozygotes had a significantly earlier age at onset compared with heterozygotes or wild types (median age at onset 3, 7, and 8 years, respectively). Of homozygotes, 60% were diagnosed with MMD before age 4, and all had infarctions as the first symptom. Infarctions at initial presentation and involvement of posterior cerebral arteries, both known as poor prognostic factors for MMD, were of significantly higher frequency in homozygotes than in heterozygotes and wild types. Variants other than c.14576G>A were not associated with clinical phenotypes.

Conclusions: The homozygous c.14576G>A variant in *RNF213* could be a good DNA biomarker for predicting the severe type of MMD, for which early medical/surgical intervention is recommended, and may provide a better monitoring and prevention strategy. ***Neurology*® 2012;78:803–810**

GLOSSARY

CI = confidence interval; **HRM** = high-resolution melting; **MMD** = moyamoya disease; **OR** = odds ratio; **PCA** = posterior cerebral artery.

Moyamoya disease (MMD) is a cerebrovascular disease, which is now a relatively common cause of pediatric strokes.[1,2] Annual incidence is estimated to be 0.35–0.54 per 100,000 person-years in Japan[3,4] and about one tenth of that in Europe.[5,6] MMD can lead to devastating neurologic deficits and intellectual impairments if left untreated.

Although MMD is a progressive disease, its natural history varies from slow progression to rapid neurologic decline.[7] Preoperative infarctions, early age at onset, intellectual impairment, seizure, and progressive posterior cerebral artery (PCA) stenosis are known prognostic factors.[8–11] Surgical revascularization can improve the cerebrovascular hemodynamics and prevent subsequent attacks in the ischemic type of MMD.[8] Thus, early diagnosis and surgical intervention are very important.

Genetic factors underlying MMD are of clinical relevance. Epidemiologic studies have shown that about 15% of patients had a family history.[12] Anticipation of the disease is

Supplemental data at www.neurology.org

Supplemental Data

From the Department of Human Genetics (S.M., N.M., A.N.-T., Y.K., I.O., Y.T., H.D., H.Sakai, H.Saitsu, N.M.), Yokohama City University Graduate School of Medicine, Yokohama; Touho Neurosurgical Clinic (H.T.), Osaka; Tokyo Women's Medical University Institute for Integrated Medical Sciences (K.S., T.Y.), Tokyo; Department of Neurosurgery (M.H., N.K.), Yokohama City University Graduate School of Medicine, Yokohama; Department of Neurosurgery (H.K., K.N.), Tone Chuo Hospital, Gunma; Division of Medical Genetics (N.O.), Osaka Medical Center and Research Institute for Maternal and Child Health, Osaka; Department of Rehabilitation Medicine (T.M.), Ichikawa City Rehabilitation Hospital, Ichikawa; Department of Clinical Neurology and Stroke Medicine (S.K., Y.K.), Yokohama City University Graduate School of Medicine, Yokohama; Department of Biostatistics and Epidemiology (M.T., S.M.), Yokohama City University Medical Center, Yokohama; Department of Medical Genetics (Y.M.), Tohoku University School of Medicine, Sendai; Department of Pediatrics (S.K.), Tohoku University School of Medicine, Sendai, Japan.

Disclosure: Author disclosures are provided at the end of the article.

Copyright © 2012 by AAN Enterprises, Inc.

Copyright © by AAN Enterprises, Inc. Unauthorized reproduction of this article is prohibited.

Table 1 Sample demographics of patients with moyamoya disease and controls[a]

Clinical features	No. of patients (%)	No. of patients without data
MMD	204	
Gender (M/F)	68 (33.5)/135 (66.5)	1
Distribution of age at onset	0–58 y	7
Frequency of childhood onset (<15 y)	143 (72.6)	
Frequency of childhood onset (<4 y)	36 (18.3)	
Clinical manifestation		11
Infarction	87 (45.1)	
TIA	77 (39.9)	
ICH/IVH	17 (8.8)	
Others	12 (6.2)	
With family history	41 (20.1)	0
With intellectual impairment	33 (17.7)	18
With epilepsy	33 (17.6)	16
PCA involvement		52
Unilateral	31 (20.4)	
Bilateral	43 (28.3)	
Total	74 (48.7)	
Bilateral MMD	148 (96.1)	50
Controls	283	
Gender (M/F)	140 (51.5):132 (48.5)	11

Abbreviations: ICH/IVH = intracranial hemorrhage/intraventricular hemorrhage; MMD = moyamoya disease; PCA = posterior cerebral artery; TIA = transient ischemic attack.
[a] Numbers of patients (%) in each feature are shown, except for the distribution of ages at onset for all patients.

also observed in familial MMD.[13] Recently, the important MMD susceptibility gene, *RNF213*, was identified.[14,15] However, its clinical relevance remains unknown. For this investigation, we conducted a comprehensive genetic study of *RNF213* as well as a clinical phenotype analysis of MMD.

METHODS

Study subjects. Blood samples from 204 Japanese patients with MMD were obtained consecutively between January 2008 and February 2011. There were no sample overlaps between ours and those in the previous studies.[14,15] MMD was diagnosed as either definite (bilateral) or probable (unilateral) according to published guidelines.[16] Six patients with probable MMD were female adults and 5 of them had sporadic MMD. The medical charts were completed by the clinicians who were blinded to the genotype of the patients. Sample demographics are shown in table 1. We also obtained either blood or saliva samples from 62 pairs of parents, as well as 4 fathers and 13 mothers whose partners were unavailable. As many as 94 to 283 samples from healthy Japanese individuals were tested as normal controls for each sequence variant found.

Standard protocol approvals, registrations, and patient consents. Experimental protocols were approved by the Committee for Ethical Issue at Yokohama City University School of Medicine. Written informed consents were obtained from all the patients or their parents.

Mutation screening. Genomic DNA was obtained from peripheral blood leukocytes using QuickGene-610L (Fujifilm, Tokyo, Japan) or from saliva using Oragene DNA (DNA Genotek, Kanata, Canada). DNA was amplified using GenomiPhi version 2 (GE Healthcare, Buckinghamshire, UK). Mutation analysis of exons and exon-intron borders covering the coding region of *RNF213* (GenBank accession number, NM_020914.4), except for exon 61, was performed in all MMD patient samples by high-resolution melting (HRM) analysis on a LightCycler 480 System II (Roche Diagnostics, Basel, Switzerland). Primer sequences, PCR conditions, and HRM settings are available on request. HRM analysis with and without the spike-in method was performed for the detection of homozygous mutations.[17] If samples showed any aberrant melting curve patterns, direct sequencing was performed using an ABI Genetic Analyzer 3100 or 3500xL (Applied Biosystems, Foster City, CA) and analyzed with sequence analysis software version 5.1.1 (Applied Biosystems) and Sequencher 4.10 build 5828 (GeneCodes Corporation, Ann Arbor, MI). For exon 61, which bears the c.14576G>A variant, direct sequencing was performed for all patients with MMD and their parental samples. Additional screenings by HRM analysis were performed for the confirmed mutations in up to 283 normal control Japanese individuals. All variants were confirmed with PCR direct sequencing using either genomic DNA or another DNA, amplified with GenomiPhi separately. No discrepancy was seen in the data between the 2 different conditions of DNA.

Statistical analysis. Patients without information for each clinical feature (listed below) were excluded from the analyses (table 1 and tables e-2 and e-3 on the *Neurology*® Web site at www.neurology.org). All statistical analyses were performed using SPSS Statistics 19 (IBM, New York, NY) software. χ^2 tests were applied to compare each categorical phenotype variable between different genotypes: clinical symptom at onset, with/without family history, intellectual impairment, epilepsy, and the unilateral/bilateral distribution of vasculopathy. Non-normally distributed continuous variables, such as age at onset and the number of steno-occlusive PCA arteries were compared using the Mann-Whitney *U* test and Kruskal-Wallis test between different genotypes. $p < 0.05$ was considered statistically significant. A Kaplan-Meier curve was used to assess the cumulative incidence with the log-rank test. The Cox regression model was used to test which variables were associated with age at onset. The exact 95% confidence interval (CI) of the incidence rate of MMD was calculated according to the binomial distribution. The comparisons of clinical features between parent-offspring pairs or sibling pairs were performed using the Wilcoxon signed-rank test and McNemar test.

RESULTS

Identification of *RNF213* variants. c.14576G>A was identified in 39 of 41 patients with familial MMD (95.1%), in 129 of 163 patients with nonfamilial MMD (79.2%), and in 5 of

Copyright © by AAN Enterprises, Inc. Unauthorized reproduction of this article is prohibited.